Available online at www.sciencedirect.com
SCIENCE DIRECT®
Polymer 44 (2003) 6789–6806
polymer
www.elsevier.com/locate/polymer

The heat capacity signal from modulated temperature DSC in non-isothermal conditions as a tool to obtain morphological information during reaction-induced phase separation

Steven Swier, Bruno Van Mele*

Department of Physical Chemistry and Polymer Science, Faculty of Applied Sciences Pleinlaan 2, Vrije Universiteit Brussel—VUB, Polymer Science—FYSC (TW), B-1050 Brussels, Belgium

Received 29 January 2003; received in revised form 28 July 2003; accepted 4 August 2003

Abstract

Thermal properties of materials formed during reaction-induced phase separation (RIPS) of modified epoxy–amines can be obtained from the derivative of the heat capacity signal (dC_p/dT) in non-isothermal conditions following a certain cure schedule. A method is proposed in which the dC_p/dT signal is deconvoluted, resulting in values of T_g and ΔC_p at T_g, which can be used as probes for the composition and fraction of each phase, respectively. The following modified epoxy–amine systems, showing LCST-type demixing behavior, are presented: (i) the linearly polymerizing system diglycidyl ether of bisphenol A (DGEBA) + aniline; (ii) the network-forming system DGEBA + methylenedianiline (MDA) both modified with the high-T_g thermoplastic poly(ether sulphone) (PES: $T_g = 223$ °C) and (iii) DGEBA + MDA modified with the low-T_g copolymer poly(ethylene oxide)-*block*-poly(propylene oxide)-*block*-poly(ethylene oxide) (triblock: $T_g = -70$ °C). The onset of RIPS can be detected before the cloud point for systems (i) and (ii), indicating that the dC_p/dT signal is sensitive to phases in the sub-micron scale. Evolutions of the composition and fraction as a function of conversion during RIPS in isothermal conditions contribute to the understanding of the relation between the cure schedule and the morphological development. For the network-forming systems (ii) and (iii), overlapping peaks in the dC_p/dT signal reveal complex phase structures with interphases arising in certain cure conditions. The network structure in combination with limited interdiffusion rates results in fixation of the morphology in the former system. On the contrary, higher interdiffusion rates gives rise to a better segregation between the PES-rich and epoxy–amine-rich phases in system (i).

Keywords: Modulated temperature differential scanning calorimetry; Reaction-induced phase separation; Interphase

1. Introduction

Reaction-induced phase separation (RIPS) of a modified, homogeneous epoxy–amine mixture takes place as a result of the increase in molecular weight of the reactive species during cure. This thermodynamic driving force for phase separation has to be considered together with the kinetics of interdiffusion between the initiated coexisting phases to understand the morphology development [1–3]. The interplay between the rate of phase separation and the reaction rate has to be understood as a function of processing parameters such as the cure temperature (T_{cure}) and time (or conversion) in order to design these high performance resins [4]. To tune these events, selection of the epoxy–amine chemistry in view of reactivity, full cure glass transition (T_{gfull}) and final cross-link density (X_c) has to be done in conjunction with the modifier selection. The modifier has to be compatible with the unreacted epoxy–amine, while phase separation has to occur in the course of cure. Its molecular weight and glass transition will also determine the diffusion rates and thus the kinetics of phase separation. Moreover, the conversion at gelation (x_{gel}) for a certain epoxy resin should be compared to the conversion at the onset of phase separation (x_{ps}) at T_{cure} [1,5,6]. Vitrification of either or both the coexisting phases will interfere with the development of phase separation and freeze in a thermodynamically unstable morphology. Knowledge of the glass transition of the epoxy–amine-rich and modifier-rich phase with respect to T_{cure} is therefore

* Corresponding author. Tel.: +32-2-629-3288; fax: +32-2-629-3278.
E-mail address: bvmele@vub.ac.be (B. Van Mele).

0032-3861/$ - see front matter © 2003 Elsevier Ltd. All rights reserved.
doi:10.1016/j.polymer.2003.08.009

crucial. The glass transitions of these constituents are directly linked to the composition of both coexisting phases. A technique capable of detecting changes in composition and fraction of these phases as a function of conversion during RIPS is very valuable in view of processing optimization. Moreover, the reaction rate of the modified epoxy resin also depends on the concentration of the functional groups in each phase [7–9].

Ex situ microscopic techniques like SEM and TEM have been widely used to monitor morphological changes at discrete times during cure or after reaction completion [10–12]. While the 'structure' and fraction of both phases can be determined in this way, at least semi-quantitatively, no direct information about their composition can be obtained. Recent studies obtained compositional changes by using energy dispersive spectroscopy at the interphase between an epoxy–amine and poly(vinylpyrrolidone) [13,14]. Micro-Raman spectroscopy can also be used to detect changes in thermoplastic content locally [15].

In situ morphological development has usually been investigated with light scattering techniques, providing information on the onset of phase separation (cloud point), the phase separation mechanism (nucleation and growth or spinodal decomposition) and the evolution of the periodic distance during cure [16,17]. While the amount of scattering is determined by the composition of both phases and its constituents, the composition cannot be easily obtained, and complications arise when the refractive indexes of the coexisting phases are similar or evolve to similar values during cure [18,19]. In situ dielectric spectroscopy can provide the onset of phase separation using the interfacial polarization between both phases, while vitrification of these phases during cure can also be detected [20–22]. Dynamic rheometry can detect these chemorheological changes in situ on the basis of changes in the (complex) viscosity during RIPS. Whether the epoxy or the thermoplastic constitutes the matrix can be determined from the change in viscosity at the cloud point [23]. Dynamic mechanical thermal analysis has also been shown to be mostly influenced by phase continuity [24]. A particulate or inverted morphology could be distinguished from the ratio of the heights of tan delta peaks [25].

Modulated temperature DSC can detect the reaction rate in the non-reversing heat flow signal and chemorheological changes like vitrification in the heat capacity and heat flow phase signal simultaneously and in situ during RIPS [26,27]. The effect of phase separation in modified epoxy–amine systems is measured in an indirect and postponed way as vitrification of a high-T_g poly(ether sulphone) (PES) phase [27] or as an increase in reaction rate due to concentration of reactive groups [9]. An excess contribution in the heat capacity signal, corresponding to heat effects associated with phase separation, provides a direct way to detect RIPS in the low-T_g (triblock) copolymer poly(ethylene oxide)-*block*-poly(propylene oxide)-*block*-poly(ethylene oxide) [9]. Thermal properties of heterogeneous epoxy systems as developed in isothermal or non-isothermal cure schedules can be obtained in post-cure experiments from the heat capacity signal, and, especially, its derivative to temperature (dC_p/dT) [9,28]. Moreover, possible residual reaction exothermicity and enthalpic relaxation effects are found in the non-reversing heat flow signal.

A peak resolution technique based on Gaussian functions has been developed for the dC_p/dT signal to obtain phase weight fractions for interpenetrating polymer networks [24,29]. This strategy will be explored in this work to obtain *quantitative* information about the fraction of the epoxy–amine-rich and thermoplastic-rich phases from dC_p/dT. Moreover, evolutions in compositions can be calculated from the T_g of both phases and possible interphases present. Both the high-T_g (amorphous) PES-modified and the low-T_g (semi-crystalline) triblock copolymer will be used to study the effect of changing interdiffusion rates on the morphological evolution. Apart from the network-forming system diglycidyl ether of bisphenol A (DGEBA) + methylenedianiline (MDA), the high-T_g modifier will also be used together with the DGEBA + aniline system, forming a linear macromolecule. This last system simulates the behavior of a polymer blend in which the molecular weight of one of the components is changed. While fixation of the heterogeneous structure by the epoxy cross-links is expected for the network-forming system, this can be excluded for the DGEBA + aniline system.

2. Experimental

2.1. Materials

A bifunctional epoxy, diglycidyl ether of bisphenol A (DGEBA, Epon825 from Shell) with an epoxy equivalent weight (EEW) of 180 g equiv.$^{-1}$ was used in combination with an appropriate amount of a bifunctional amine (aniline from Fluka) or a tetrafunctional amine hardener (methylenedianiline, MDA from Janssen Chimica) with amine equivalent weights of 46.5 g equiv.$^{-1}$ and 49.5 g equiv.$^{-1}$, respectively. Different mixtures of these pure systems were prepared with 20 wt% of poly(ethersulphone) (PES from Aldrich: $M_w = 20,000$ g mol^{-1}; $T_g = 223$ °C) and with 50 wt% of the triblock copolymer poly(ethylene oxide)-*block*-poly(propylene oxide)-*block*-poly(ethylene oxide) (from Aldrich: $M_n = 4400$ g mol^{-1} with 30 wt% ethylene oxide; $T_g = -70$ °C [9]). To obtain a homogeneous mixture of the high-T_g modified DGEBA + aniline, PES was first dissolved in the epoxy using CH_2Cl_2, which was evaporated at about 120 °C under extensive stirring followed by vacuum evaporation at 100 °C. Aniline was mixed afterwards for about 5 min at 80 °C. For the network system, the appropriate quantities of all components (DGEBA + MDA/PES) were dissolved in CH_2Cl_2/CH_3OH (99/1), followed by solvent evaporation at 40 and 80 °C under vacuum for 1 h

and 5 min, respectively. The DGEBA + MDA/triblock system was mixed at 80 °C for 5 min. All these preparation methods reduce the amount of preliminary reaction to a minimum.

2.2. Techniques

Cure experiments on the PES-modified systems were performed on a TA Instruments 2920 DSC with MDSC™ option and a refrigerated cooling system (RCS, lowest initial temperature: −65 °C). Helium was used as a purge gas (25 ml min^{-1}). Indium and cyclohexane were used for temperature calibration. The former was also used for enthalpy calibration. Heat capacity calibration was performed with a PMMA standard (supplied by Acros) using the heat capacity difference between two temperatures, one above and one below the glass transition temperature of PMMA [30], to make sure that heat capacity changes were adequately measured. For quantitative heat capacity measurements at temperatures below −50 °C, a temperature-dependent C_p calibration was used. This consists of measuring the heat capacity evolution of a reference material over the whole temperature range of interest and calculating a heat capacity calibration factor as a function of temperature [31]. Cure was performed in hermetic aluminum pans (TA Instruments) with sample weights between 5 and 10 mg. Modulation conditions were: amplitude of 1 °C and a 60 s period. Cloud points were detected by measuring the light transmitted through thin samples (held between glass slides) in a Mettler Toledo FP82HT hot stage equipped with a photodetector. A Spectratech optical microscope was used (magnification of 4).

A TA Instruments Q1000 with an RCS cooling unit was used in the case of the triblock modifier since the new cell and cooler design allow for the lower initial temperatures needed to study this system (minimum: −90 °C). The Q1000 DSC cell uses Tzero™ technology. Nitrogen was used as a purge gas (25 ml min^{-1}), and hermetic crucibles were used with sample weights ranging from 5 to 10 mg.

3. Results and discussion

3.1. Composition and fraction of coexisting phases as obtained from the dC_p/dT signal

The glass transition (T_g) of a homogeneous blend of two components can be predicted with the Couchman equation when the T_g and the heat capacity change at T_g ($\Delta C_p(T_g)$) of both constituents are known together with their composition in the blend [32]. This is shown for homogeneous mixtures of DGEBA + PES in Fig. 1. No phase separation or reaction was detected in the range of temperatures used to determine the T_gs of these systems. Indeed, the LCST for DGEBA + PES was found to be 241 °C [33]. Since a close correspondence is seen with the simulation (compare line with (●) in Fig. 1), the Couchman equation can be used as a tool to determine the composition in an unknown homogeneous mixture. Moreover, the glass transition of unreacted mixtures of DGEBA + aniline with PES can also be predicted by assuming a binary mixture of the epoxy–amine species with PES ((○) in Fig. 1).

This concept was used in the present work to determine the composition of the coexisting phases during RIPS. For this purpose, the modified epoxy–amine system is considered to be a binary mixture of the modifier and the epoxy–amine species. This means that differential segregation of the epoxy and amine in both phases is a priori excluded.

To confirm this assumption, three modified epoxy–amine systems were investigated at appropriate isothermal cure temperatures: (i) DGEBA + aniline/20 wt% PES at 100 °C, (ii) DGEBA + MDA/20 wt% PES at 80 °C and (iii) DGEBA + MDA/50 wt% triblock copolymer at 90 °C. In these conditions, the conversion at which phase separation initiates, x_{ps}, is 67 and 37% as determined by optical microscopy measurements for systems (i) and (iii), respectively [9]. No cloud point could be detected in this way for system (ii), a finding probably related to the proximity of the refractive indexes of both phases [19]. Vitrification of the PES-rich phase for system (ii) has been measured [27], however, and occurs at 51%. By using a mechanistic model for the reaction kinetics [34,35], the residual concentrations of aniline and MDA (A_1) can be estimated to be about one-fifth of the initial concentration at 67 and 37%, respectively. Thus, the majority of amine functionalities are already attached to the epoxy (A_2 and A_3) at x_{ps} and will diffuse as one species. Further confirmation for the fact that differential segregation is unlikely in these systems can be obtained by comparing the reaction enthalpy ($\Delta_r H$) of modified with unmodified systems, normalized per mole epoxy and by assuming stoichiometric compositions. $\Delta_r H$ measured in both isothermal and non-isothermal conditions for systems (i), (ii) and (iii) is (-107 ± 6) kJ mol^{-1}, (-104 ± 4) kJ mol^{-1} and (-105 ± 6) kJ mol^{-1}, respectively. Note that systems (i) and (ii) were previously analyzed in isothermal conditions, for which comparable reaction enthalpies were found [27]. The values reported here are close to those found for stoichiometric mixtures of DGEBA + aniline, (-105 ± 2) kJ mol^{-1}, and for DGEBA + MDA, (-104 ± 3) kJ mol^{-1} [36]. Deviations from the stoichiometric composition during RIPS would result in a fraction of unreacted functional groups and thus lower values of $\Delta_r H$. Other studies on the effect of the (PES) modifier content on $\Delta_r H$ also confirm that the epoxy–amine ratio in the coexisting phases is the same [37,38].

Thus, in the absence of differential segregation, phase i can be considered to be a homogeneous mixture of the epoxy–amine, having the (stoichiometric) start composition, and the modifier. A model based on thermodynamic considerations was initially presented by Couchman to

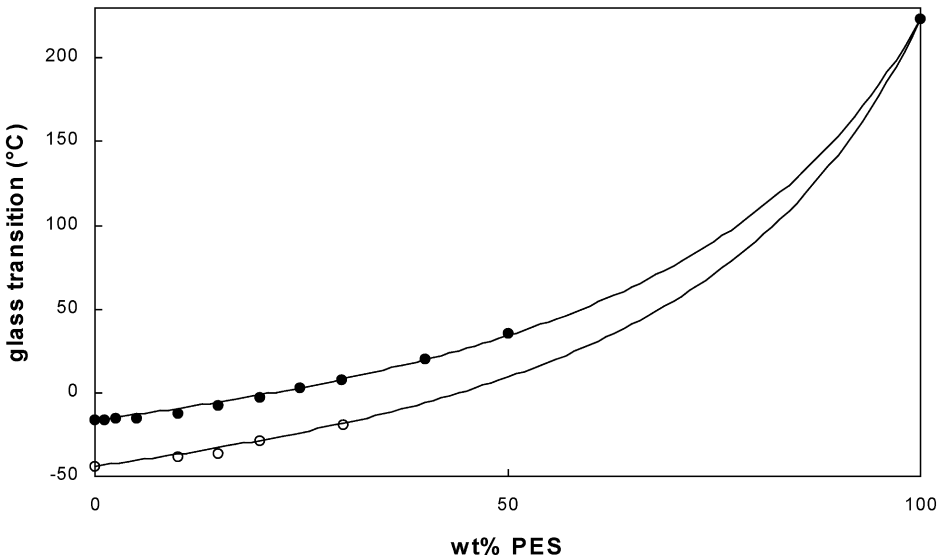

Fig. 1. Glass transition as a function of wt% of PES for homogeneous mixtures of DGEBA + PES (●) and of DGEBA + aniline/PES (○); parameters for the Couchman equation: $T_{g\mathrm{DGEBA}} = -16.3$ °C; $\Delta C_{p\mathrm{DGEBA}}(T_g) = 0.54$ J g^{-1} K^{-1}; $T_{g\mathrm{DGEBA+aniline}}(x=0) = -41$ °C; $\Delta C_{p\mathrm{DGEBA+aniline}}(x=0) = 0.52$ J g^{-1} K^{-1}; $T_{g\mathrm{PES}} = 223$ °C; $\Delta C_{p\mathrm{PES}}(T_g) = 0.21$ J g^{-1} K^{-1}; simulation with the Couchman equation [31] (—).

calculate the T_g of polymer blends [39]. This approach can be applied here by considering a blend of the epoxy–amine species with the modifier. Since the epoxy–amine species changes during reaction, the thermal properties of this component have to be introduced at the attained conversion x: 'global' conversion x assumes that x is the same in all existing phases. This will be a reasonable approximation in the early stages of RIPS, while large differences in reaction rate and thus conversion development are expected in the later stages of RIPS (see later discussions). Simulation of the reaction rate in heterogeneous conditions, based on the information gathered in this work, will serve as a validation of the stated assumptions [38].

$$\ln T_{g,i}(x) = \frac{w_{\mathrm{EPAM},i}\Delta C_{p\mathrm{EPAM}}(T_{g\mathrm{EPAM}}(x))\ln T_{g\mathrm{EPAM}}(x) + (1 - w_{\mathrm{EPAM},i})\Delta C_{p\mathrm{MOD}}(T_{g\mathrm{MOD}})\ln T_{g\mathrm{MOD}}}{w_{\mathrm{EPAM},i}\Delta C_{p\mathrm{EPAM}}(T_{g\mathrm{EPAM}}(x)) + (1 - w_{\mathrm{EPAM},i})\Delta C_{p\mathrm{MOD}}(T_{g\mathrm{MOD}})} \quad (1)$$

where $w_{\mathrm{EPAM},i}$ is the weight fraction of the epoxy–amine in phase i; $T_{g\mathrm{MOD}}$ and $\Delta C_{p\mathrm{MOD}}(T_{g\mathrm{MOD}})$ are the thermal properties for pure modifier (PES or triblock) (see Table 1); $T_{g\mathrm{EPAM}}(x)$ and $\Delta C_{p\mathrm{EPAM}}(T_{g\mathrm{EPAM}}(x))$ are, respectively, the T_g and heat capacity change at T_g of the epoxy–amine calculated at the reaction conversion x, as measured with MTDSC in Refs. [34,35]. When $T_{g,i}$ is known, Eq. (1) can be used to obtain the composition of the epoxy–amine in phase i. x can be obtained from partial integration of the non-reversing heat flow signal. The above-mentioned agreement between $\Delta_r H$s for modified and unmodified systems means that full cure conditions can be reached for all modified systems. Also note that the use of the

The heat capacity change determined at the glass transition of phase i ($\Delta C_{p,i}(T_{g,i}(x))$) is related to the weight fraction of that phase Φ_i in the mixture, as can be expressed by making the mass balance and by assuming that heat capacity changes are additive:

$$\Delta C_{p,i}(T_{g,i}(x)) = (w_{\mathrm{EPAM},i}\Delta C_{p\mathrm{EPAM}}(T_{g,i}(x)) + (1 - w_{\mathrm{EPAM},i})\Delta C_{p\mathrm{MOD}}(T_{g,i}(x)))\Phi_i \quad (2)$$

Table 1
Input data for Eqs. (1) and (2) required to calculate $w_{\mathrm{EPAM},i}$ and Φ_i from knowledge of $T_{g,i}(x)$ (°C) and $\Delta C_{p,i}(T_g(x))$ (in J g^{-1} K^{-1}); the input for the $T_{g\mathrm{EPAM}} - x$ relationship and $\Delta C_{p\mathrm{EPAM}}(T_{g\mathrm{EPAM}}(x))$ is taken from Refs. [33,34]

	$T_{g\mathrm{MOD}}$	$\Delta C_{p\mathrm{MOD}}(T_{g\mathrm{MOD}})$	$\Delta C_{p\mathrm{MOD}}(T_{g,i}(x))$
PES	223	0.21	$-8.8\times10^{-4}T_{g,i} + 0.40$
Triblock	−70	0.65	$-1.1\times10^{-3}T_{g,i} + 0.58$

	T_{g0}	$T_{g\mathrm{full}}$	$\Delta C_{p\mathrm{full}}/\Delta C_{p0}$	λ	$\Delta C_{p\mathrm{EPAM}}(T_{g\mathrm{EPAM}}(x))$
DGEBA + aniline($r=1$)	−41	95	0.97	0.62	$-6.9\times10^{-2}x^2 + 1.2\times10^{-2}x + 0.52$
DGEBA + MDA($r=1$)	−16	175	0.58	1.00	$-1.8\times10^{-1}x^2 - 1.1\times10^{-1}x + 0.55$

where $\Delta C_{p\mathrm{EPAM}}(T_{g,i}(x))$ and $\Delta C_{p\mathrm{MOD}}(T_{g,i}(x))$ are the heat capacity changes for the epoxy–amine and the modifier at $T = T_{g,i}(x)$, respectively. ΔC_p versus composition plots showed deviations from linearity when interactions between both components were present [40]. However, no significant interactions in the current systems have been reported in literature [37,41].

Input data for Eqs. (1) and (2) are summarized in Table 1. $\Delta C_{p\mathrm{EPAM}}(T_{g,i}(x))$ can be obtained by extrapolating the temperature dependence of the heat capacity in the liquid state $C_{pl}(T)$ and that in the glassy state $C_{pg}(T)$ for a pure epoxy–amine at $T_{g\mathrm{EPAM}}(x)$ to $T = T_{g,i}(x)$. This rigorous method can be simplified by realizing that $C_{pl}(T)$ and $C_{pg}(T)$ do not change considerably as a function of conversion, especially in the conversion range of interest (x_{ps} is 37% or higher as stated above) [34,35]. Thus, $\Delta C_{p\mathrm{EPAM}}(T_{g,i}(x))$ can be obtained from $\Delta C_{p\mathrm{EPAM}}(T_{g\mathrm{EPAM}}(x))$ where x corresponds to $T_{g\mathrm{EPAM}}$ equal to $T_{g,i}$. $\Delta C_{p\mathrm{PES}}(T_{g,i}(x))$ has been obtained experimentally from the heat capacity signal in MTDSC. Both $C_{pl}(T)$ and $C_{pg}(T)$ correspond well to literature data for this thermoplastic [42]. Since cold crystallization and melting occur during heating of the triblock copolymer (see also Section 3.4), $C_{pl}(T)$ cannot be obtained experimentally over the entire temperature range. Therefore, calculated literature data for poly(ethylene oxide) and poly(propylene oxide) [42] have been used in weight fractions of 30 and 70%, respectively, corresponding to the composition of the poly(ethylene oxide)-*block*-poly(propylene oxide)-*block*-poly(ethylene oxide) modifier (see also Section 2). The value of $\Delta C_{p,\mathrm{triblock}}(T_g)$ calculated at T_g equal to -70 °C, corresponds to the experimental value.

$T_{g,i}$, $\Delta C_{p,i}$ and the width of the glass transition region of phase i ($\Delta T_{g,i}$) will be obtained from the dC_p/dT signal using a peak resolution technique based on Gaussian functions [24,28,29]:

$$G_i = \frac{\Delta C_{p,i}}{\Delta T_{g,i}(\pi/2)^{1/2}} \exp\left(-\frac{2(T - T_{g,i})^2}{(\Delta T_{g,i})^2}\right) \quad (3)$$

with G_i in J mol^{-1} K^{-2}. Note that $\Delta T_{g,i}$ obtained in this way corresponds to the width of the Gaussian peak at half height. This method is based on the notion that the dC_p/dT versus temperature signal of a pure polymer can be described by one Gaussian function [43].

The result of the deconvolution approach is given for a DGEBA + MDA/20 wt% PES system cured at 80 °C for 100 min (Fig. 2), corresponding to the initiation of RIPS in this system (see Section 3.3). Since the temperature dependency of C_p in the liquid state is less steep than that in the glassy state, a non-constant baseline was used to correct the dC_p/dT curve as elaborated upon in Ref. [44].

While two resolved glass transitions are difficult to obtain from the heat capacity signal, dC_p/dT clearly contains two (overlapping) peaks, corresponding to a low-T_g, epoxy–amine-rich α-phase and a high-T_g, PES-rich β-phase. The evolution of composition and fraction of these phases will be considered separately in Section 3.

Finally, the mass balance can be used to check the obtained values for $w_{\mathrm{EPAM},i}$ and Φ_i :

$$\sum_i (w_{\mathrm{EPAM},i}\Phi_i) = w_{\mathrm{EPAM,hom}}, \qquad \sum_i \Phi_i = 1 \quad (4)$$

with $w_{\mathrm{EPAM,hom}}$ the weight fraction of epoxy–amine in the initial, homogeneous mixture.

3.2. PES-modified linearly polymerizing DGEBA + aniline system

Homogeneous mixtures of DGEBA + aniline/20 wt% PES are cured for different times at 100 °C and subsequently analyzed in non-isothermal post-cure experiments (Fig. 3) to obtain the residual reaction exothermicity and the heat capacity evolution as a function of temperature. An increase in reaction rate is seen when the initial conversion increases from 0 to 53%, as can be concluded from the shift to lower temperatures of the onset and maximum ((●) in Fig. 3) in the non-reversing heat flow signal. A higher initial concentration of hydroxyl groups is responsible for this effect since they catalyze the epoxy–amine reaction [45,46]. The heat capacity and dC_p/dT evolutions reflect the transition from a homogeneous (0–53%) to a heterogeneous (63–87%) mixture. The reaction exothermicity partly overlaps with the glass transition region in the higher conversion range, illustrating the benefit of using MTDSC for this system. Since this residual reaction occurs at the end of the glass transition region, the evolution in the heat capacity signal still reflects the material formed in the preceding isothermal cure. Using this signal to study the thermal properties formed during RIPS at 100 °C is therefore permitted.

The result of the peak resolution analysis on the dC_p/dT evolutions (shown in Fig. 3) is given in Fig. 4 for a wide range of conversions. A single T_g is found until x reaches 63%, indicating a homogeneous mixture. The presence of PES ($T_g = 223$ °C, see Table 1) increases this T_g by about 17 °C in comparison to the unmodified DGEBA + aniline mixture (compare (□) with line in Fig. 4). A much higher ΔT_g, as obtained from the deconvolution method (Eq. (3)), is also found for the modified system (□) in comparison to the unmodified epoxy–amine (×) and pure PES ($\Delta T_{g\mathrm{PES}} = 7$ °C). The broadness of the glass transition region has been interpreted as an indication of miscibility. Weak interactions in a polymer–polymer blend were found to give rise to this borderline miscibility, indicating that miscibility on a molecular scale is not necessarily achieved [47]. At $x = 63\%$ two glass transitions are found, marking the onset of RIPS. Note that the cloud point as measured by optical microscopy occurs about 5% later (dashed line in Fig. 4), indicating that T_g is sensitive to the presence of smaller phase sizes (order of magnitude of 10 nm [48]). The small size of these phases implies a high fraction of

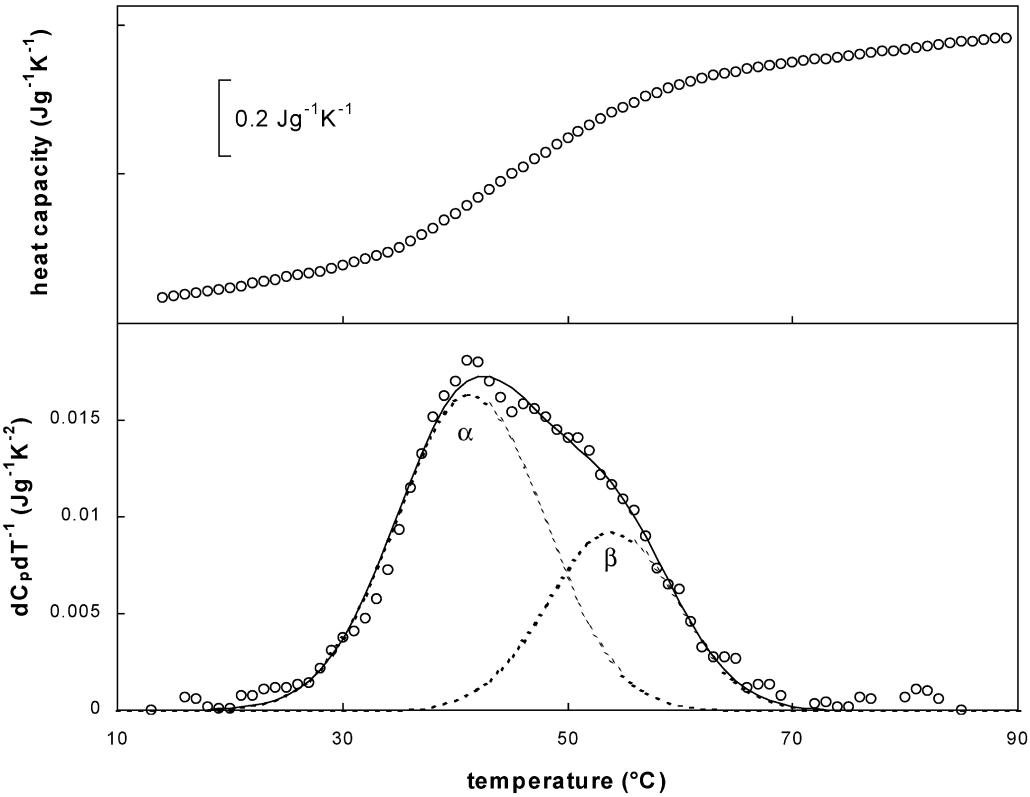

Fig. 2. Heat capacity and derivative of the heat capacity signal to temperature (dC_p/dT) for the 20 wt% PES-modified, stoichiometric DGEBA + MDA system cured for 100 min at 80 °C (○); separate Gaussian peaks (Eq. (3) (- - -) together with their sum (—); results from the deconvolution (α-phase: epoxy–amine-rich phase, β-phase: PES-rich phase): $T_{g,\alpha} = 41.9$ °C; $T_{g,\beta} = 54.9$ °C; $\Delta T_{g,\alpha} = 14.2$ °C; $\Delta T_{g,\beta} = 11.4$ °C; $\Delta C_{p,\alpha} = 0.30$ J g^{-1} K^{-1}; $\Delta C_{p,\beta} = 0.12$ J g^{-1} K^{-1}.

interphase, which cannot be deduced since both T_gs formed at $x = 63\%$ are close to each other. Another possible explanation for the higher cloud point conversion is the small difference in refractive index between the coexisting phases, as revealed by their small difference in composition. The evolutions of these compositions can be obtained from the Couchman relation (Eq. (1)) and are shown in Fig. 5.

The T_g of the epoxy–amine-rich phase (termed α phase, $T_{g,\alpha}$) is close but slightly higher than the T_g of the unmodified DGEBA + aniline system. The α phase, therefore, is almost pure in the epoxy–amine species. Further confirmation is found from the ΔT_g of this phase, which decreases with x from the onset of phase separation and evolves to the trend of the unmodified system. The difference between the T_g of the PES-rich phase (termed β phase, $T_{g,\beta}$) and $T_{g,\alpha}$ increases with x, corresponding to an enrichment of this phase in PES (see Fig. 5). Since $T_{g,\beta}$ is close to T_{cure}, especially considering $\Delta T_{g,\beta}$ ((●) in Fig. 4), diffusion of the epoxy–amine out of the β phase is restricted. As evidenced by the heat capacity change, vitrification of this phase initiates at around 80% and is complete at 95%, where phase separation is no longer possible. ΔT_g decreases strongly in this conversion region, indicating that a higher fraction of the β phase becomes frozen in, while further reaction and thus RIPS of the fraction that is still mobile results in a narrower glass transition region [35]. Thus, a considerable amount ($w_{EPAM,\beta} > 0.50$) of the epoxy–amine species remains in the β phase, while the α phase is almost pure in this component.

The fraction Φ of both phases has been calculated from the heat capacity change at T_g of the α and β phases ($\Delta C_{p,\alpha}$ and $\Delta C_{p,\beta}$, respectively) and Eq. (2) (see Fig. 5).

Initially, Φ_β is higher than Φ_α, while diffusion of the epoxy–amine species towards the α phase increases its fraction. This trend can also be obtained visually by applying the lever rule in the composition graph in Fig. 5 (dashed line), confirming that a binary mixture arises during RIPS with the α and β phases as the major phases. A final value of 0.67 is found for Φ_α, smaller than the theoretical value for a pure epoxy–amine phase (0.80), a finding which can be ascribed to a combination of vitrification of the β phase, trapping some epoxy–amine species, and to the shape of the phase diagram. Indeed, while the epoxy–amine-rich branch can be expected to be near pure epoxy–amine, the PES-rich branch will gradually evolve to purer PES as temperature and x rise [9].

Further indications for the shape of the phase diagram can be obtained by studying the effect of T_{cure} on the composition of both phases. For this purpose, mixtures of DGEBA + aniline/20 wt% PES were analyzed isothermally at different cure temperatures until reaction

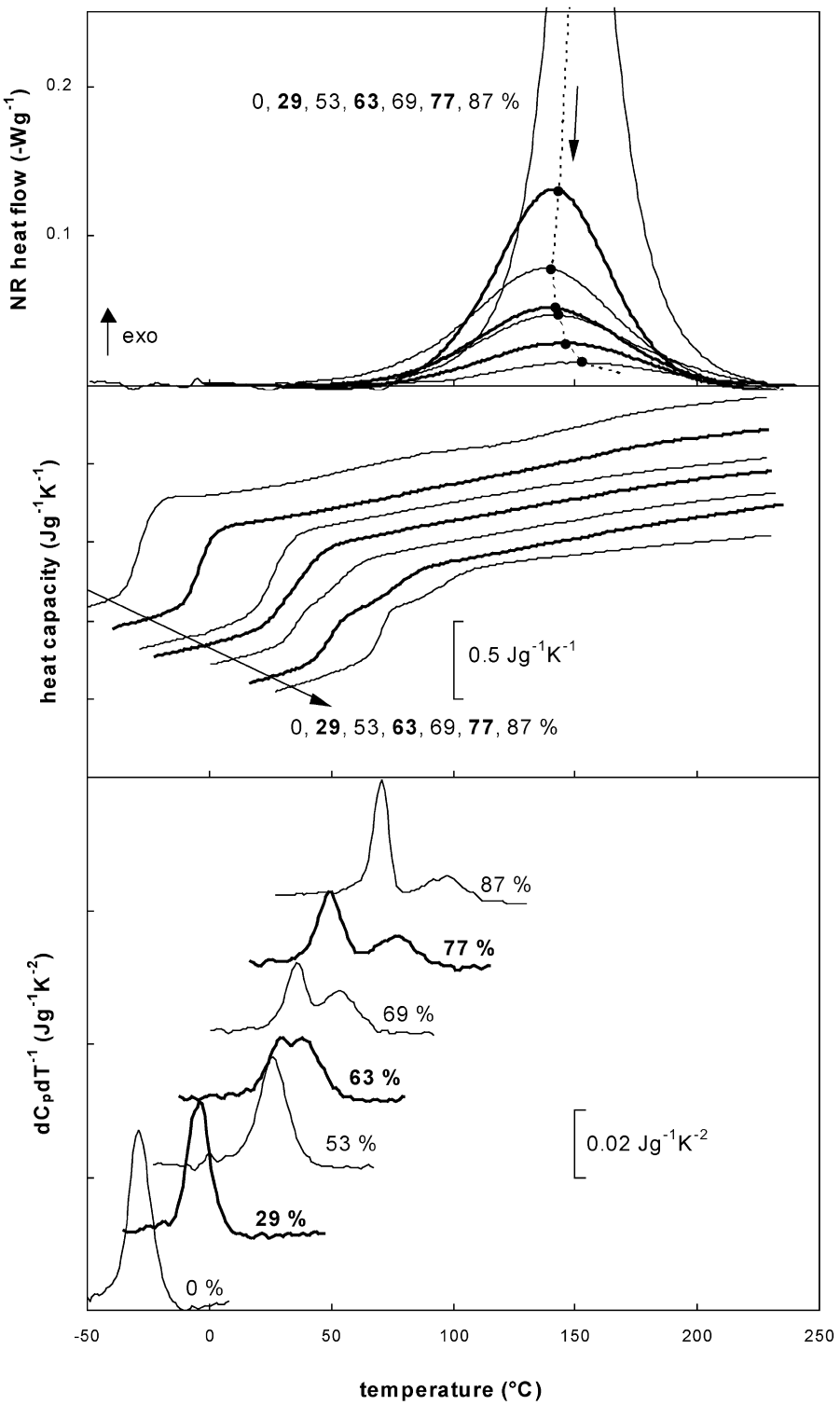

Fig. 3. Non-reversing heat flow (second heating was used as a baseline), heat capacity and derivative of the heat capacity signal to temperature (dC_p/dT) for the 20 wt% PES-modified, stoichiometric DGEBA + aniline system during heating at 2.5 °C min^{-1} after isothermal cure for different times at 100 °C; conversions reached after these times are indicated; the maximum in the non-reversing heat flow (●) (not shown for 0%).

completion was reached (from the non-reversing heat flow signal) and until no more phase separation was noticed (from the heat capacity signal). The conversion attained at this point equals 88% for cure at 60 °C and reaches 100% at 260 °C. A state diagram is shown in Fig. 6, reflecting the composition of the α and β phases reached by a combination of thermodynamic and kinetic factors. Note that data points for T_{cure} above 130 °C were obtained by performing a two-step cure schedule to reduce excessive heat production.

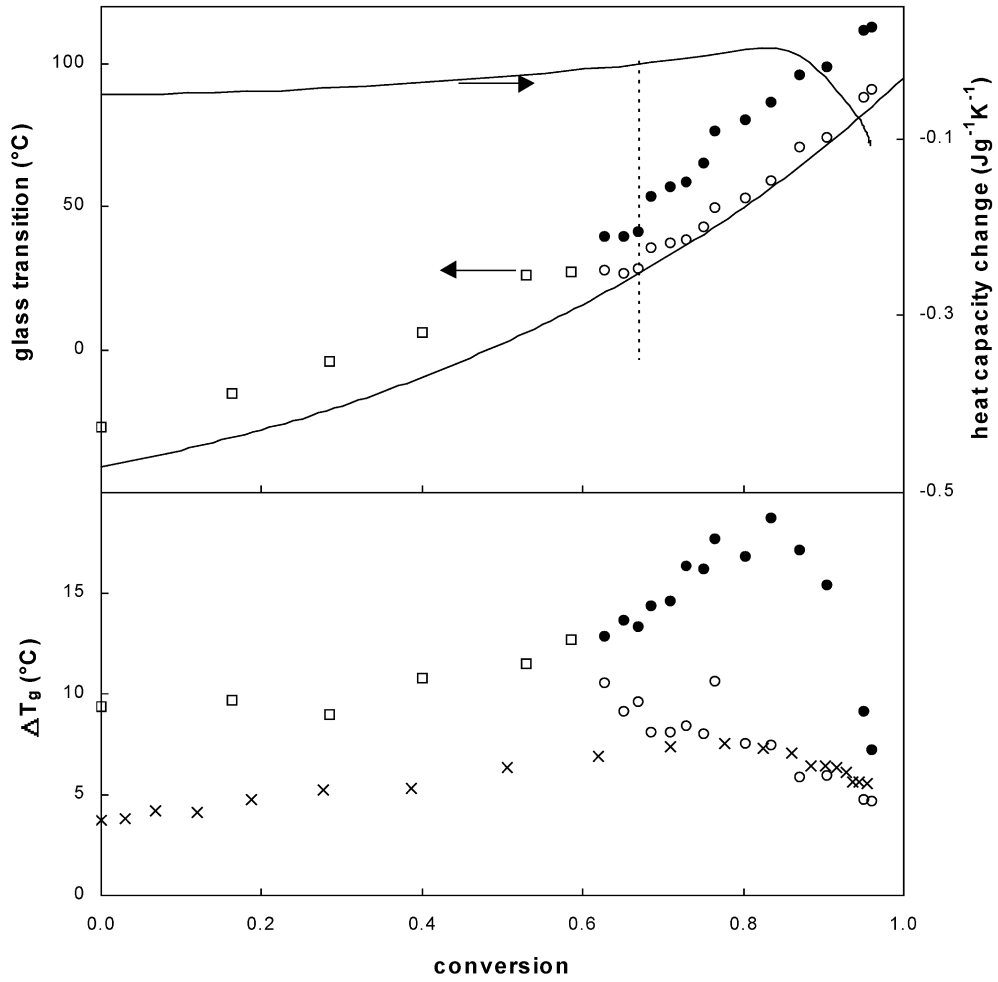

Fig. 4. Glass transition and width of the glass transition region ΔT_g as a function of conversion for a stoichiometric DGEBA + aniline mixture modified with 20 wt% PES and cured at 100 °C using different cure times; the evolution of the heat capacity change with conversion during the isothermal cure at 100 °C is also shown for comparison; $T_g - x$ relationship for unmodified DGEBA + aniline (—); T_g and ΔT_g of cure conditions exhibiting one glass transition (□) together with the epoxy–amine-rich (α phase, ○) and the PES-rich (β phase, ●) phase for heterogeneous cure conditions; ΔT_g for the unmodified DGEBA + aniline mixture (×); the cloud point as measured by optical microscopy (- - -, [9]).

A higher T_{cure} clearly results in enrichment of the β phase in PES, while the α phase is pure in the epoxy–amine species from about 120 °C. At 260 °C, the β phase still contains about 5% of the epoxy–amine. Note that the phase compositions reached at this temperature can be attained by including a final thermal treatment at 260 °C for samples cured at any preceding isothermal cure temperature. Thus, phase morphologies are not frozen in irreversibly after isothermal cure for this system. Since a linear macromolecule is formed during the DGEBA + aniline reaction, the fully reacted modified system corresponds to a polymer blend. Fig. 6 also confirms the absence of differential segregation during RIPS: since $T_{g,\alpha}$ is close to T_{gfull} (95 °C) in all conditions (or α phase is pure in the epoxy–amine species), no deviations from the stoichiometric composition takes place in the α phase. Indeed, small deviations from this composition would already result in a significant drop of $T_{g,\alpha}$ as was elaborated upon in Refs. [34,35].

3.3. PES-modified network-forming DGEBA + MDA system

The evolution of the composition and fraction of both phases during RIPS was analyzed at 80 °C for the DGEBA + MDA/20 wt% PES system. The non-isothermal post-cure experiments on this system after different reaction times at 80 °C are shown in Fig. 7. As was the case in the linear epoxy system (Fig. 3), the non-reversing heat flow shows a reaction rate increase after the initial conversion stages (0–45%). The heat capacity signal (C_p) and, especially, dC_p/dT characterizes the glass transition regions of the homogeneous (23, 37%) and heterogeneous (from 45%) materials (below 100 °C). The residual reaction exotherms become asymmetric from around 60% since the T_g of the system, attained in the preceding isothermal cure step, acts as a physical barrier: the residual reaction only starts when the necessary mobility is regained upon going through the glass transition region [49]. The highest x

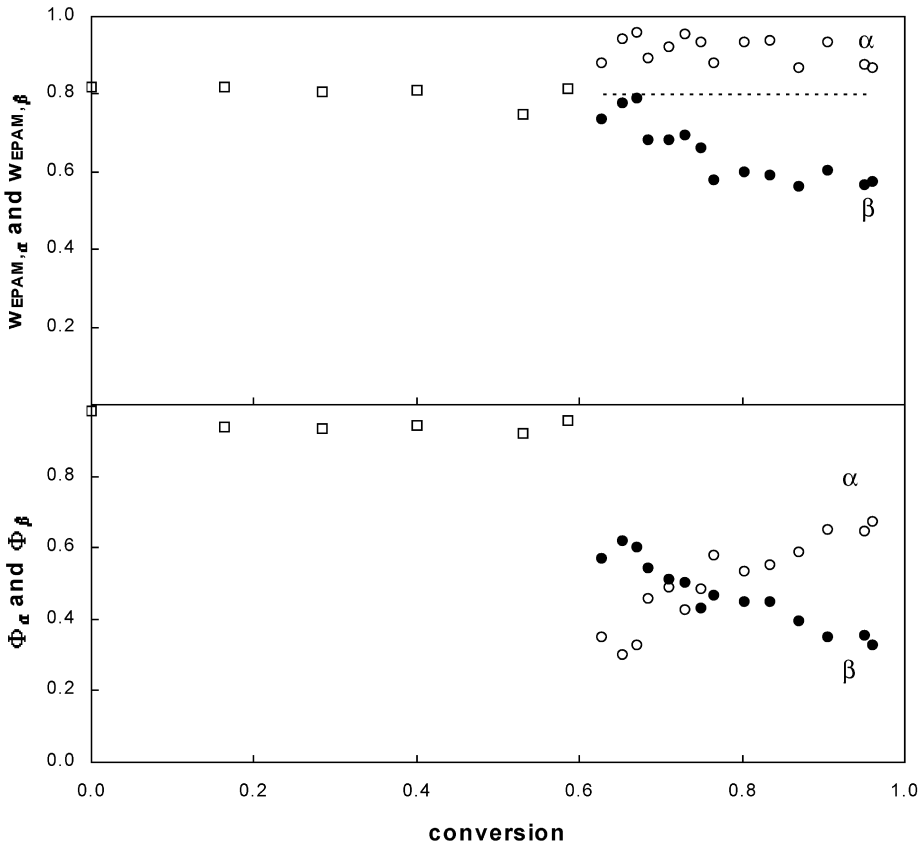

Fig. 5. Composition ($w_{EPAM,\alpha}$ and $w_{EPAM,\beta}$) and fraction (Φ_α and Φ_β) of the α (○) and β-phases (●) as a function of conversion for the isothermal cure at 100 °C of DGEBA + aniline/20 wt% PES as determined from $T_{g,\alpha}$ and $T_{g,\beta}$ (with Eq. (1) and Table 1) and from $\Delta C_{p,\alpha}$ and $\Delta C_{p,\beta}$ (with Eq. (2) and Table 1), respectively; the mass balances were checked with Eq. (4) $\sum(w_{EPAM,i}\Phi_i) = 0.78 \pm 0.03$ and $\sum\Phi_i = 0.97 \pm 0.04$.

analyzed (75%) corresponds to a system cured for 400 min at 80 °C, where an extended diffusion-controlled reaction occurs in isothermal conditions (more than 200 min, not shown). The decreased reaction rate and the slow variation of T_g result in structural relaxation (endothermic peak in Fig. 7, 75%) [50].

An additional shoulder, which was not present in the linear modified epoxy system, occurs above 150 °C in the

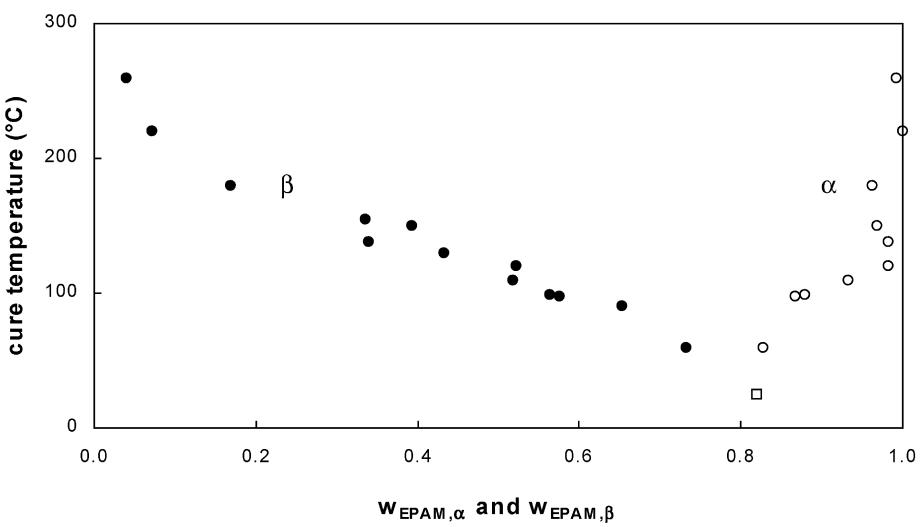

Fig. 6. Cure temperature as a function of composition ($w_{EPAM,\alpha}$ and $w_{EPAM,\beta}$) for DGEBA + aniline/20 wt% PES mixtures cured until no further reaction (no more change in the non-reversing heat flow signal) or phase separation (no more change in the heat capacity signal) occurred; homogeneous system at 25 °C (□); α phase (○) and β phase (●); the mass balances were checked with Eq. (4): $\sum(w_{EPAM,i}\Phi_i) = 0.77 \pm 0.05$ and $\Phi_i = 0.98 \pm 0.09$.

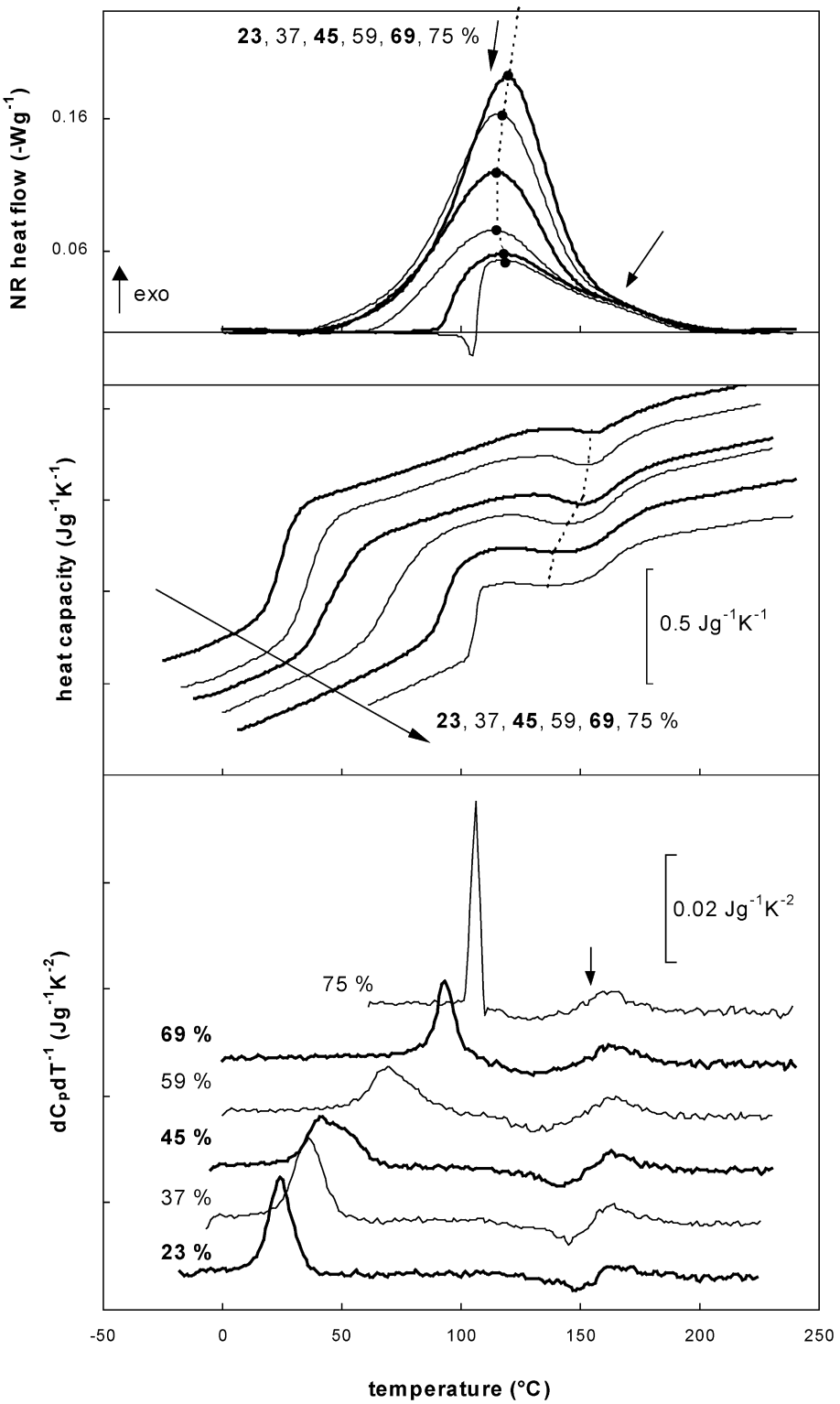

Fig. 7. Non-reversing (NR) heat flow (second heating was used as a baseline), heat capacity (C_p) and derivative of the heat capacity signal to temperature (dC_p/dT) for the 20 wt% PES-modified, stoichiometric DGEBA + MDA system during heating at 2.5 °C min^{-1} after isothermal cure for different times at 80 °C; conversions reached after these times are indicated; the maximum in the non-reversing heat flow (●); the minimums in the C_p signal (attributed to the occurrence of vitrification followed by devitrification) are connected (- - -).

non-reversing heat flow (arrow in Fig. 7). This effect was also absent for the unmodified stoichiometric DGEBA + MDA system subjected to the same cure schedule (isothermal and non-isothermal) [35]. Further reaction and RIPS in the modified system will, however, result in a T_g increase of the PES-rich phase, rising above the increasing T_{cure} during the heating scan at 2.5 °C min^{-1}. The resulting vitrification is seen as a step-wise decrease in C_p. When T_{cure} again increases above T_g, devitrification is seen. A comparison can be made here with the partially miscible polymer blend poly(ethylene oxide)/PES, for which a high-T_g PES-rich phase arises during temperature-induced phase separation also resulting in (partial) vitrification and subsequent devitrification effects [51,52]. The minimum in C_p is shown in Fig. 7 (dashed line) and translates into a downward and upward peak in the dC_p/dT signal (arrow). Thus, the shoulder in the non-reversing heat flow indicates further reaction in diffusion-controlled conditions in the PES-rich phase.

Note that the last step-wise increase in the heat capacity signal has been, incorrectly, attributed to the high-T_g phase formed during the preceding isothermal cure for DGEBA + MDA/poly(sulphone) [53].

The peak resolution analysis is applied to the dC_p/dT signal below 100 °C to make sure that only the morphology formed during the preceding isothermal cure is analyzed (Fig. 8). As in the linear system, the T_g of the homogeneous system (conversions till 45%) is higher than that of the unmodified system due to the presence of PES. While no phase separation for any conversion could be detected with optical microscopy in this system, the occurrence of two phases can be distinguished from 45% with dC_p/dT. A study using model compounds for the epoxy–amine species demonstrated that demixing indeed occurs in DGEBA + MDA modified with the similar thermoplastic poly(sulphone) [54].

The proximity of T_{cure} to $T_{g,\alpha}$ and $T_{g,\beta}$ has drastic effects on the phase separation kinetics: interdiffusion is highly restricted after the initial formation of the coexisting phases. Vitrification of the PES-rich phase (β phase) occurs close to the onset of phase separation as evidenced by the relaxation in the heat flow phase (onset around 51%, indicated by first dotted line in Fig. 8). This can also be concluded from the evolution of $T_{g,\beta}$ and $\Delta T_{g,\beta}$: while no vitrification is expected at the onset of phase separation (45%: $T_{g,\beta} + \Delta T_{g,\beta} = 66\ °C < T_{cure}$), interference clearly initiates around 50%. At this point, the β phase will be partly frozen in. Further phase separation accompanied by diffusion of the epoxy–amine species to the α phase will therefore be limited. Indeed, no considerable change is noticed in the composition and fraction of both phases after the onset of phase separation. Thus, while further reaction takes place in both phases (increase in $T_{g,\alpha}$ and $T_{g,\beta}$), phase separation is halted.

Finally, vitrification of the α phase is initiated around 65%, as revealed by the shoulder in the relaxation peak of the heat flow phase (second dotted line in Fig. 8) and the sharp drop in ΔT_g. A remarkable effect is seen at this point: one T_g is found ((×) in Fig. 8) while the system is still in the two-phase region of the phase diagram. This can be explained by further reaction of the α phase whereas the β phase is essentially frozen in. At some point, $T_{g,\alpha}$ will thus rise up to $T_{g,\beta}$, resulting in an 'apparent' homogeneous system. At this stage, the glass transition region cannot be used anymore to study the evolving morphology.

The difference in diffusion rates between the network-forming, modified system and the linearly polymerizing one can also be illustrated by performing an additional thermal treatment at 260 °C on samples cured for different times at 80 °C (Fig. 9). A comparable combined cure schedule on the latter system resulted in the same end material: an α phase pure in epoxy–amine and a β phase almost pure in PES (see Section 3.2).

dC_p/dT as a function of temperature for the DGEBA + MDA/20 wt% PES system cured for 100 min at 80 °C and thermally treated at 260 °C for 20 min is shown in Fig. 10. In comparison to the situation after only the isothermal cure (see Fig. 7), an extra phase can be distinguished. Note that the phase richest in the epoxy–amine species and in the modifier will be, respectively, termed α and β phases throughout this work. The interphase γ turns out to contain about the same amount of epoxy–amine ($w_{EPAM,\gamma}$ around 0.85 in Fig. 9) as the α phase in isothermal conditions ($w_{EPAM,\alpha}$ around 0.87 in Fig. 8). The α phase formed after the thermal treatment at 260 °C is pure in the epoxy–amine species and probably arises from the higher interdiffusion rates at this temperature.

A large amount of epoxy–amine remains in the β phase as the conversion, reached at 80 °C, increases (Fig. 9). After 50% of reaction at 80 °C, $w_{EPAM,\beta}$ no longer changes considerably during the additional thermal treatment at 260 °C. Thus, the highly branched, high M_w epoxy–amine formed at 80 °C and the high-T_g PES are unable to diffuse between the β phase and the α or γ phases. Lower conversions at 80 °C still allow diffusion to occur at 260 °C. Since reaction and thus formation of the final network also takes place quickly at this temperature and would interfere with additional diffusion, the apparent temperature dependence of the diffusion rate seems to be higher than that of the reaction rate.

The fact that the network fixes the morphology, therefore freezing in a thermodynamically unstable system, was illustrated for DGEBA + MDA modified with 50 wt% PES and for other modified thermosets [9] and has also been concluded from morphological studies in literature [1,10,14,33,55]. Most of these studies performed RIPS at a T_{cure} much higher than 80 °C (typical range from 150 to 260 °C) resulting in phase separation on a larger scale (typically 2–5 μm [10]).

On the other hand, lower T_{cure}s were analyzed for the system DGEBA + MDA/poly(sulphone) with SEM,

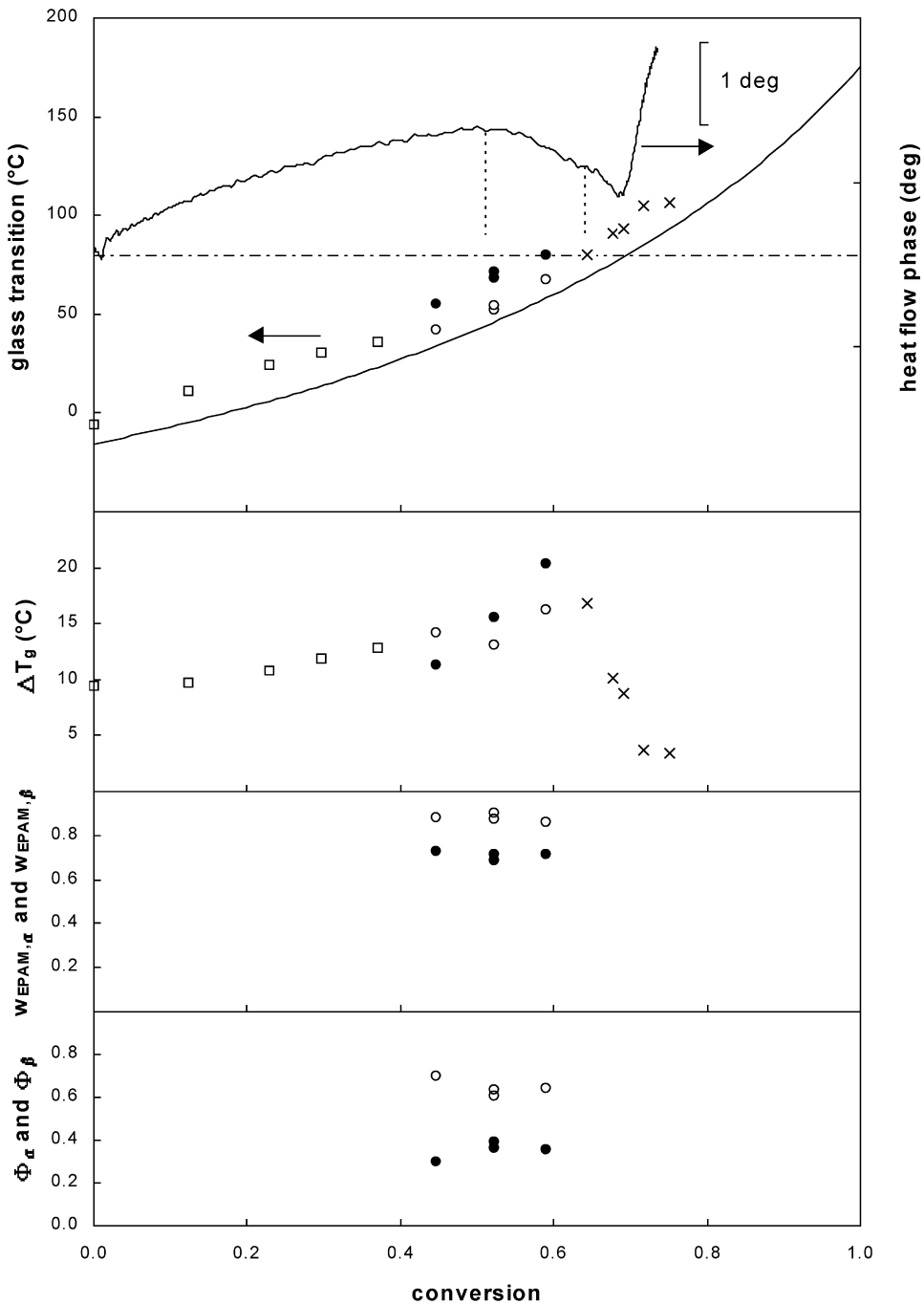

Fig. 8. T_g, ΔT_g, $w_{EPAM,\alpha}$, $w_{EPAM,\beta}$, Φ_α and Φ_β as a function of conversion for a stoichiometric DGEBA + MDA mixture modified with 20 wt% PES and cured at 80 °C using different cure times; the evolution of the heat flow phase with conversion during the isothermal cure at 80 °C is shown for comparison (see text) together with the onset of vitrification of the α phase (epoxy–amine-rich) and the β phase (PES-rich) (dotted line); $T_g - x$ relationship for unmodified DGEBA + MDA (—); homogeneous systems exhibiting one glass transition (□); the epoxy–amine-rich (α phase, ○) and the PES-rich (β phase, ●) phase for heterogeneous systems; the 'apparent' homogeneous systems (×); T_{cure} is indicated for reference (— - — -); the mass balances were checked with Eq. (4): $\sum(w_{EPAM,i}\Phi_i) = 0.78 \pm 0.09$ and $\sum\Phi_i = 0.97 \pm 0.09$.

showing that at 100 °C very small particles were formed (0.2–0.3 μm), while no RIPS could be detected at 60 °C [41]. RIPS in the present system was also investigated at T_{cure} lower than 80 °C and showed that below 60 °C, phase separation could no longer be detected in dC_p/dT. Considering that x_{ps} at 80 °C is 45% and the maximum x reached at 60 °C is 62%, RIPS is expected to be thermodynamically possible at 60 °C. However, lower diffusion rates probably result in an even smaller separation of the α and β phases as in the case of T_{cure} at 80 °C (Fig. 8).

The information contained in Fig. 9 is potentially interesting for designing cure schedules aimed at PES-modified network systems with tailor-made morphologies.

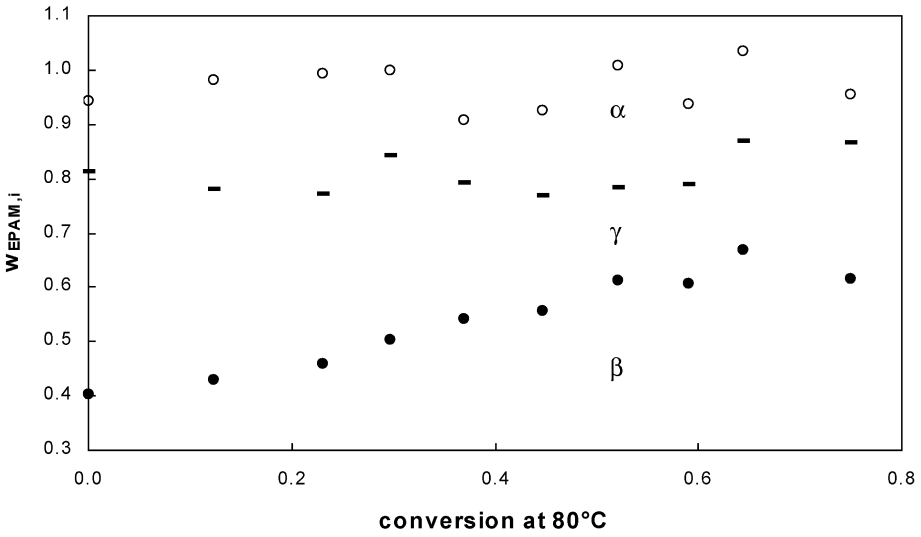

Fig. 9. $w_{EPAM,\alpha}$ (○), $w_{EPAM,\beta}$ (●) and $w_{EPAM,\gamma}$ (−) as a function of conversion at 80 °C for the DGEBA + MDA/20 wt% PES system attained after an additional thermal treatment at 260 °C for 20 min; the mass balances were checked with Eq. (4) $\sum(w_{EPAM,i}\Phi_i) = 0.79 \pm 0.07$ and $\sum\Phi_i = 1.01 \pm 0.09$.

3.4. DGEBA + MDA modified with the low-T_g triblock copolymer

To increase the diffusion rates during phase separation, the low-T_g triblock copolymer poly(ethylene oxide)-*block*-poly(propylene oxide)-*block*-poly(ethylene oxide) was used as a modifier for DGEBA + MDA. A homogeneous mixture of DGEBA + MDA/50 wt% triblock was cured for different times at 90 °C and subsequently treated non-isothermally as shown in Fig. 11. While reaction was re-initiated close to devitrification of the material formed isothermally in the case of the PES-modified systems (see Figs. 3 and 7), a larger gap is noticed for the triblock modified system.

Only in the higher conversion range (75, 83%), the non-reversing heat flow indicates reaction close to the high-T_g epoxy–amine-rich phase. In this x range at 90 °C, the final stages of RIPS are reached. At this point, the semi-crystalline triblock copolymer will be almost pure in its phase (see also Fig. 12).

Cold crystallization and melting therefore take place (heating at 1 °C min^{-1}), seen as an exothermic and endothermic peak, respectively (indicated by (△) and (◇) in the non-reversing heat flow of Fig. 11). Note that the crystallization and melting heat, as calculated from the total heat flow, are found to be equal (absolute values around 1 J g^{-1}), indicating that no crystallization occurs during the fast cooling from 90 to −90 °C. This means that the glass transition region, as measured below the onset of cold crystallization, reflects a fully amorphous material, and fractions calculated for the triblock-rich phases are correct. Note, however, that melting is also present as a positive

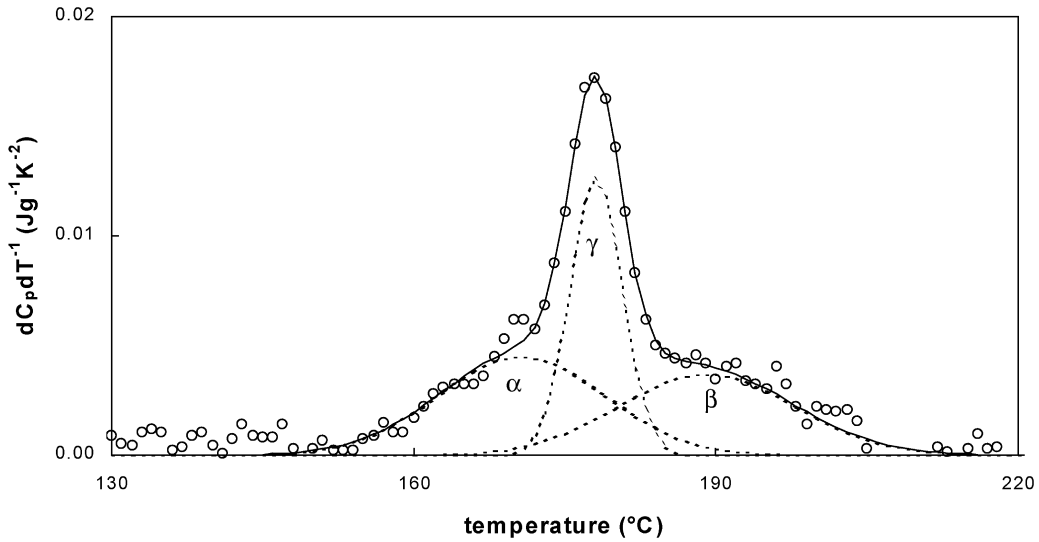

Fig. 10. Derivative of the heat capacity signal to temperature (dC_p/dT) for the 20 wt% PES-modified, stoichiometric DGEBA + MDA system cured for 100 min at 80 °C, followed by a thermal treatment at 260 °C (20 min) (○); separate Gaussian peaks Eq. (3) (- - -) and their sum (—).

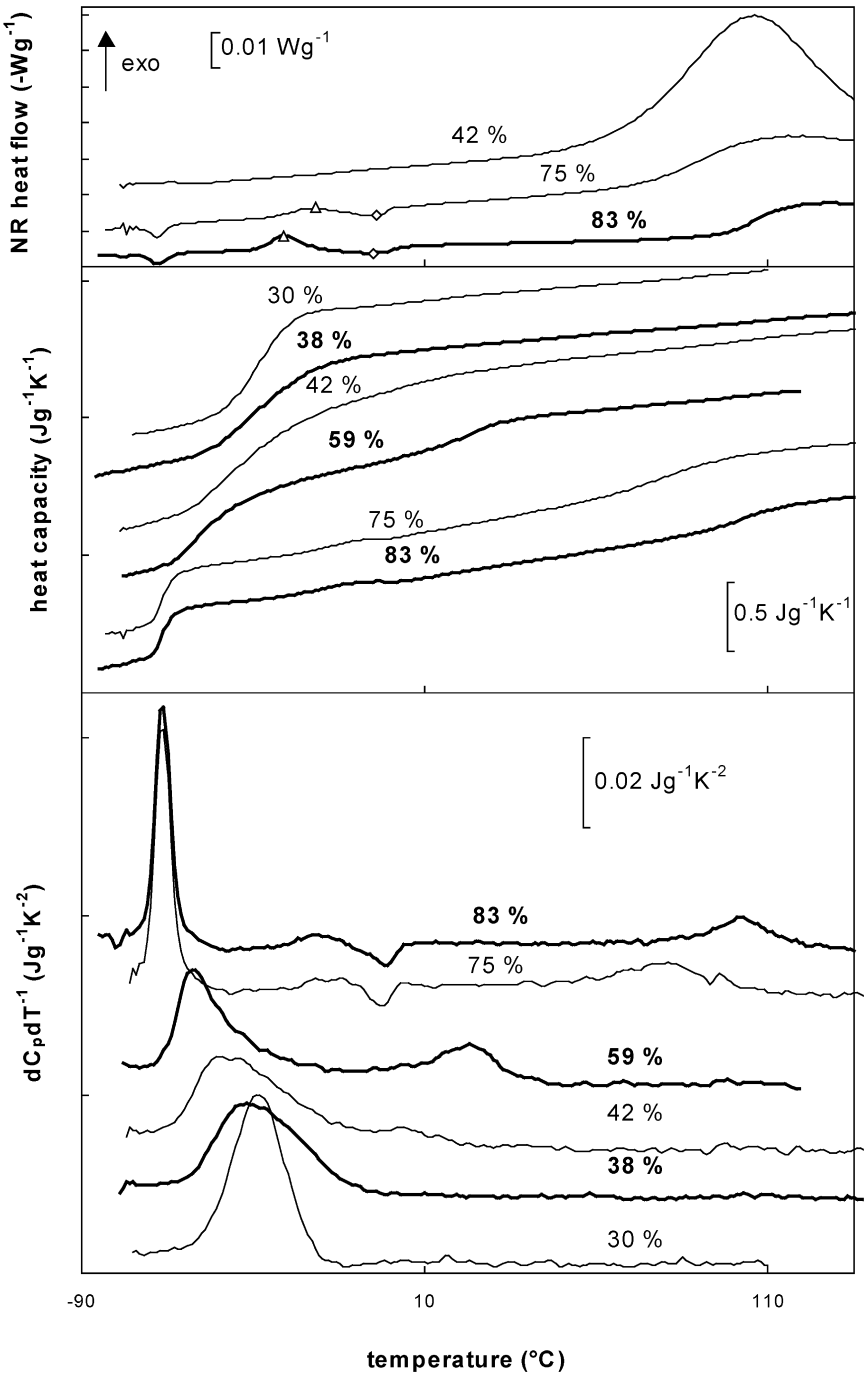

Fig. 11. Non-reversing (NR) heat flow (partly shown for a conversion of 42, 75 and 83%), heat capacity (C_p) and derivative of the heat capacity signal to temperature (dC_p/dT) for the 50 wt% triblock-modified, stoichiometric DGEBA + MDA system during heating at 1 °C min^{-1} after isothermal cure for different times at 90 °C; conversions reached after these times are indicated; cold crystallization (△) and melting (◇) peaks are indicated on the non-reversing heat flow.

peak in the heat capacity signal and as an upward and downward peak in the dC_p/dT signal. These effects are therefore not included in the peak resolution analysis.

The T_g of the homogeneous system increases slightly with x in comparison to the faster increase in the unmodified system (Fig. 12). A competition between an increase in T_g with x of the epoxy–amine species and a decrease in compatibility of the low-T_g triblock component probably results in the observed trend. RIPS occurs at 38% as concluded from the occurrence of two T_gs. This onset corresponds to the onset of the peak (excess contribution) in the heat capacity signal in isothermal conditions at 90 °C and to the cloud point from optical microscopy (shown in Fig. 12). The excess peak in the heat capacity signal was used for the first time as a direct probe for RIPS in Ref. [9]. The fact that no difference is found between the cloud point

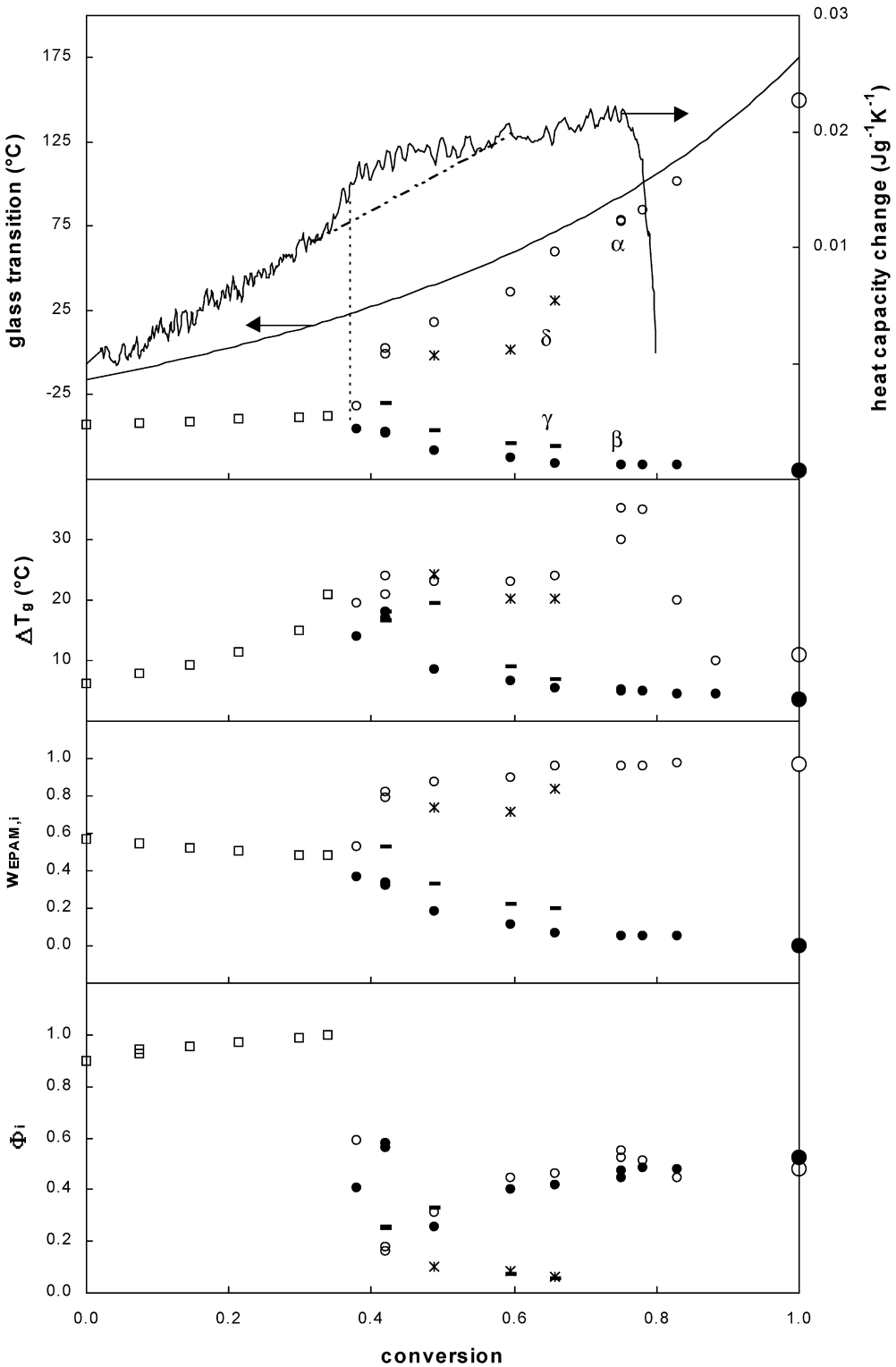

Fig. 12. Glass transition, ΔT_g, $w_{EPAM,i}$, and Φ_i as a function of conversion for a stoichiometric DGEBA + MDA mixture modified with 50 wt% triblock, cured at 90 °C; the onset of phase separation as detected by optical microscopy (- - -); the $T_g - x$ relationship for unmodified DGEBA + MDA (—); systems exhibiting one glass transition (□); the definition of phases is as in Fig. 13: α phase (○), β phase (●), γ phase ( ) and δ phase (∗); systems cured until 100% conversion by a combined cure path at 90 and 220 °C (larger symbols); the mass balances were checked with Eq. (4): $\sum(w_{EPAM,i}\Phi_i) = 0.51 \pm 0.04$ and $\sum\Phi_i = 1.06 \pm 0.09$.

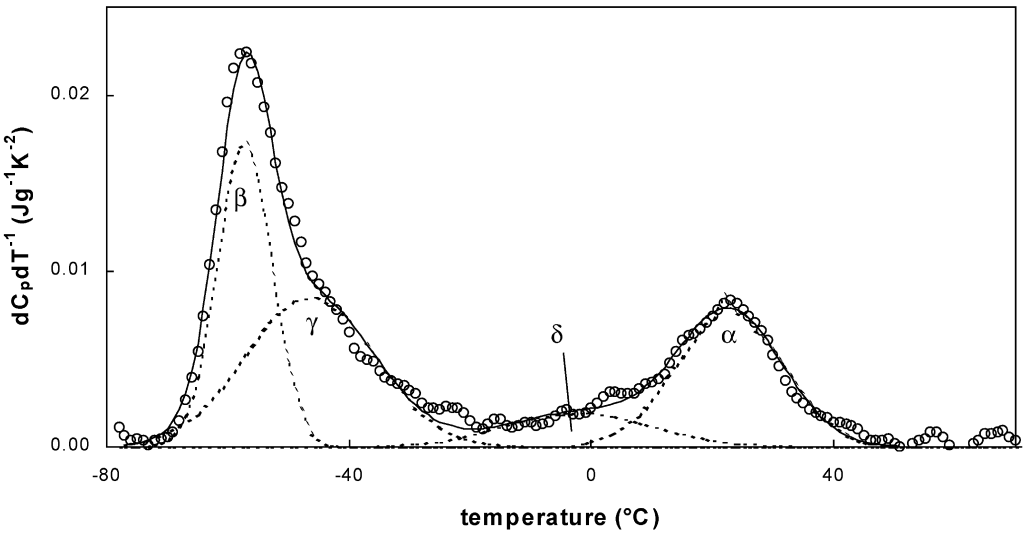

Fig. 13. dC_p/dT for the DGEBA + MDA(r = 1)/50 *wt*% triblock system cured for 135 min at 90 °C (conversion of 49%) (○); separate Gaussian peaks Eq. (3) (- - -) and their sum (—).

and the onset in the occurrence of two T_gs indicates that phases that are larger than the ones initiated in the PES-modified systems are formed. Optical micrographs indeed indicate phases in the order of magnitude of 10–20 μm after the cure at 90 °C. Both higher driving forces (thermodynamics) and higher diffusion rates (kinetics) can be held responsible for this effect. Note that indications were found that smaller phases develop for a lower T_{cure} (60 °C) [9].

A complex morphology seems to evolve beyond these initial stages. The peak resolution analysis is shown in Fig. 13 for the system cured for 135 min at 90 °C (x of 49%, not shown in Fig. 11). Apart from the epoxy–amine-rich phase (α phase) and the triblock-rich phase (β phase), two interphases γ and δ need to be considered to obtain an acceptable fit. As was the case in the PES-modified DGEBA + MDA system, the interphase constitutes a considerable part of the material. In the triblock system, the morphology is further complicated by the fact that the poly(propylene oxide) block becomes incompatible with epoxy–amines at a certain x, while the poly(ethylene oxide) block has been stated to be compatible throughout cure [56–58]. On the other hand, SAXS measurements showed that the compatibility of the latter block decreases slightly with x [59]. Indications for this compatibility decrease were also found from an increase in crystallization rate as a function of cure advancement [60]. Complex morphologies were found with large phases of 30 μm surrounded by an interphase where subinclusions in the order of 1 μm occurred [56]. Thus, the morphology corresponding to the situation after a conversion of 49% (Fig. 13) could be pictured as being composed of a phase in which PPO blocks (constitutes 70 wt% of the triblock copolymer) have self-assembled into large domains (β phase) surrounded by a large interphase with the epoxy–amine (γ phase) and the epoxy–amine-rich phase (α phase) in which the PEO blocks are interpenetrated (δ phase). One has to be cautious, however, in deciding the amount of (inter)-phases from the deconvolution analysis. At least four phases have to be considered in order to mathematically fit the dC_p/dT signal in Fig. 13. Complementary techniques are needed to attain conclusive evidence about the amount of phases, their nature and their organization in the morphology.

In contrast to the PES-modified systems, the α and β phases evolve quickly to pure epoxy–amine and triblock phases, respectively, which can be ascribed to the high interdiffusion rates caused by the low-T_g modifier. Also note that a more symmetrical evolution is found, indicating a symmetrical phase diagram, which could be related to the lower molecular weight of the triblock copolymer (4400 g mol^{-1}).

The fraction of the interphases decreases quickly (Φ_γ and Φ_δ in Fig. 12), and their presence is negligible after 70% of the reaction. RIPS is complete at this point as indicated by the purity of the α ($w_{EPAM,\alpha} = 0.97$) and β ($w_{EPAM,\beta} = 0$) phases, while further reaction of the α phase still increases $T_{g,\alpha}$. Vitrification of this phase occurs at a conversion of 83% ($T_{g,\alpha}$ = 102 °C), seen as a decrease in $\Delta T_{g,\alpha}$ and as a step-wise decrease in the (independently) obtained heat capacity signal. A post-cure experiment till 220 °C does not change the composition of both phases anymore. In contrast to the PES-modified DGEBA + MDA system, this post-cure experiment results in the same end state irrespective of the preceding cure schedule. This was tested for a T_{cure} range from 50 until 120 °C, which indicates that a highly phase separated material was already obtained in isothermal conditions. Also note that fixing of the morphology by the formed network is less probable in this system due to the much higher diffusion rate of the low-T_g component.

4. Conclusions

A peak resolution technique applied to the dC_p/dT signal from MTDSC allows the extraction of the T_g and ΔC_p of overlapping transitions, corresponding to different phases. RIPS of modified epoxy–amine systems can be analyzed in this way by using a combined isothermal and non-isothermal cure schedule. In order to use the dC_p/dT information from a non-isothermal post-cure experiment to obtain information about phases formed in the preceding isothermal cure step, additional reaction and RIPS should be avoided in the glass transition region of the induced phases. For the modified systems studied in this work, additional reaction only interferes for higher preceding conversions and around the endsets of these regions. In the case of the network-forming system modified with PES, further reaction and RIPS in non-isothermal conditions induce vitrification of the PES-rich phase beyond this point, seen as a step-wise decrease in C_p. The subsequent devitrification at higher temperatures should not be mistaken with the T_g of this phase formed in the preceding isothermal cure step. In the case of the semi-crystalline triblock modifier, cold crystallization followed by melting can also interfere. Careful selection of the temperature regions used in the peak resolution technique has to be made on the basis of this information.

Two glass transitions arise at the initiation of phase separation in all systems. In the case of the PES-modified systems, two T_gs are detected at a conversion x_{ps} prior to the cloud point conversion, while these conversions are found to coincide in the case of the triblock modifier. This indicates that smaller phases or phases with similar refractive indexes, which cannot be detected optically, are formed at x_{ps} when the high-T_g modifier is used. The large difference in (inter)diffusion rates between both modifiers can be held responsible for this observation. Beyond the onset of phase separation the composition of the α phase (epoxy–amine-rich) and the β phase (modifier-rich) evolves more quickly to the pure constituents for the low-T_g modifier. In case of the PES-modified systems, interdiffusion rates are highly restricted during isothermal cure due to the proximity of T_{cure} to $T_{g,\alpha}$ and $T_{g,\beta}$. For the DGEBA + MDA/PES system, the combination of the epoxy–amine network and the high-T_g modifier even inhibits further morphology development in an additional thermal treatment at higher temperatures. This is evidenced by the higher amount of the epoxy–amine species that remains trapped in the PES-rich phase for higher initial conversions. In contrast, both in the DGEBA + aniline/PES and in the DGEBA + MDA/triblock systems, phase separation can be induced until completion (almost pure PES and epoxy–amine phases can be formed).

For both network-forming systems, the dC_p/dT signal indicates the presence of interphase(s) in certain cure conditions. The inherent heterogeneous structure of the triblock modifier results in a complex phase morphology in the intermediate stages between the onset of phase separation and the fully phase separated material.

The sensitivity with which the dC_p/dT signal from MTDSC can analyze phases in the micron and sub-micron scale is useful in obtaining (morphological) information complementary to microscopic techniques. Moreover, the material is formed in situ in the same MTDSC experiment, and no complex sample preparation is involved. The only prerequisite is that the glass transitions of the pure constituents or the coexisting phases are different to allow for enough resolution in the dC_p/dT analysis. The evolution of the composition and fraction of coexisting phases is of interest to predict the effect of phase separation on the reaction kinetics.

References

[1] Williams RJJ, Rozenberg BA, Pascault J-P. Adv Polym Sci 1997;95:128.
[2] Kiefer J, Hilborn JG, Hedrick JL. Polymer 1996;37:5715.
[3] Rajagopalan G, Gillespie JW, McKnight SH. Polymer 2000;41:7723.
[4] Tran-Cong Q, Shibayama M. In: Araki T, editor. Structure and properties of multiphase polymeric materials. New York: Marcel Dekker; 1998.
[5] Xie X, Yang H. Mater Des 2001;22:7.
[6] Goossens JGP. Processing of tractable polymers using reactive solvents. PhD Thesis. The Netherlands: Technische Universiteit Eindhoven; 1998.
[7] Bonnet A, Pascault JP, Sautereau H, Taha M. Macromolecules 1999;32:8517.
[8] Ritzenthaler S, Girard-Reydet E, Pascault JP. Polymer 2000;41:6375.
[9] Swier S, Van Mele B. Polymer 2003;44:2689.
[10] Yamanaka K, Inoue T. Polymer 1989;30:662.
[11] Hseih HK, Su CC, Woo EM. Polymer 1998;39:2175.
[12] Oyanguren PA, Frontini PM, Williams RJJ, Vigier G, Pascault JP. Polymer 1996;37:3087.
[13] Oyama HT, Solberg TN, Wightman JP. Polymer 1999;40:3001.
[14] Oyama HT, Lesko JJ, Wightman JP. J Polym Sci: Part B 1997;35:331.
[15] van Overbeke E. PhD Thesis. Belgium; Université catholique de Louvain (UCL); 2001.
[16] Inoue T. Prog Polym Sci 1995;20:119.
[17] Maugey J, Van Nuland T, Navard P. Polymer 2001;42:4353.
[18] Kim BS, Chiba T, Inoue T. Polymer 1995;36:67.
[19] Bucknall CB, Gomez CM, Quintard I. Polymer 1994;35:354.
[20] Vinh-Tung C, Boiteux G, Seytre G, Lachenal G, Chabert B. Polym Compos 1996;17:761.
[21] Alig I, Jenninger W, Junker M, de Graaf LA. J Macromol Sci, Phys 1996;B35:563.
[22] Bonnet A, Pascault JP, Sautereau H, Rogozinski J, Kranbuehl D. Macromolecules 2000;33:3833.
[23] Meijer EH, Venderbosch RW, Goossens JGP, Lemstra PJ. High Perform Polym 1996;8:133.
[24] Hourston DJ, Song M, Schafer F-U, Pollock HM, Hammiche A. Polymer 1999;40:4769.
[25] Girard-Reydet E, Vicard V, Pascault JP, Sautereau H. J Appl Polym Sci 1997;65:2433.
[26] Swier S, Van Assche G, Van Hemelrijck A, Rahier H, Verdonck E, Van Mele B. J Therm Anal 1998;54:585.
[27] Swier S, Van Mele B. Thermochim Acta 1999;330:175.
[28] Hourston DJ, Song M, Pollock HM, Hammiche A. J Therm Anal 1997;49:209.

[29] Hourston DJ, Song M, Schafer F-U, Pollock HM, Hammiche A. Thermochim Acta 1998;324:109.
[30] Gaur U, Wunderlich B. J Phys Chem Ref Data 1982;11:313.
[31] Van Assche G, Van Hemelrijck A, Van Mele B. J Therm Anal Calorim 1997;49:443.
[32] Couchman PR, Karasz FE. Macromolecules 1978;11:117.
[33] Yoon T, Kim BS, Lee DS. J Appl Polym Sci 1997;66:2233.
[34] Swier S, Van Mele B. J Appl Polym Sci, accepted for publication.
[35] Swier S, Van Assche G, Van Mele B. J Appl Polym Sci, accepted for publication.
[36] Swier S, Van Mele B. J Polym Sci: Part B 2003;41:594.
[37] MacKinnon AJ, Jenkins SD, McGrail PT, Pethrick RA. Macromolecules 1992;25:3492.
[38] Swier S, Van Mele B. Macromolecules 2003;36:4424.
[39] Couchman PR, Karasz FE. Macromolecules 1978;11:117.
[40] Song M, Hourston DJ, Pollock HM, Hammiche A. Polymer 1999;40:4763.
[41] Martinez I, Martin MD, Eceiza A, Oyanguren P, Mondragon I. Polymer 2000;41:1027.
[42] Wunderlich B. ATHAS databank: table of the properties of 200 linear macromolecules and small molecules, url: http://web.utk.edu/~athas/databank/intro.html.
[43] Song M, Hourston DJ, Schafer F-U, Pollock HM, Hammiche A. Thermochim Acta 1997;304/305:335.
[44] Song M, Hourston DJ, Reading M, Pollock HM, Hammiche A. J Therm Anal 1999;56:991.
[45] Rozenberg BA. Adv Polym Sci 1986;75:113.
[46] Swier S, Van Mele B. Thermochim Acta, accepted for publication.
[47] Mandal TK, Woo EM. Polymer 1999;40:2813.
[48] MacKnight WJ, Karasz FE. In: Allen G, Bevington JC, editors. Comprehensive polymer science. Polymer characterization, vol. 1. New York: Pergamon Press; 1989. Chapter 4.
[49] Van Mele B, Rahier H, Van Assche G, Swier S. In: Reading M, editor. The application of MTDSC for the characterization of curing systems. The characterization of polymers using advanced calorimetric methods, Dordecht: Kluwer Academic; 2003. in press; Chapter.
[50] Wisanrakkit G, Gillham JK. J Appl Polym Sci 1991;42:2465.
[51] Dreezen G, Groeninckx G, Swier S, Van Mele B. Polymer 2001;42:1449.
[52] Swier S, Pieters R, Van Mele B. Polymer 2002;43:3611.
[53] Alig I, Jenninger W, Schawe JEK. Thermochim Acta 1999;330:167.
[54] de Graaf LA, Hempenius MA, Möller M. Polym Prepr 1995;36:787.
[55] Bucknall CB, Partridge IK. Polymer 1983;24:639.
[56] Mijovic J, Shen M. Wing Sy.J. Macromolecules 2000;33:5235.
[57] Guo Q, Thomann R, Gronski W, Thurn-Albrecht T. Macromolecules 2002;35:3133.
[58] Zheng S, Zhang N, Luo X, Ma D. Polymer 1995;36:3609.
[59] Lipic PM, Bates FS, Hillmyer MA. J Am Chem Soc 1998;120:8963.
[60] Swier S, Cools S, Van Mele B. Unpublished results.